Inorganic Chemistry

Article

pubs.acs.org/IC

Thorium Terephthalates Coordination Polymers Synthesized in Solvothermal DMF/H_2O System

Clément Falaise, Jean-Sébastien Charles, Christophe Volkringer,* and Thierry Loiseau

Unité de Catalyse et Chimie du Solide (UCCS) − UMR CNRS 8181, Université de Lille, USTL-ENSCL, Bat C7, BP 90108, 59652 Villeneuve d'Ascq, France

Supporting Information

ABSTRACT: A series of thorium-based terephthalates have been solvothermaly synthesized in *N*,*N*-dimethylformamide (DMF) with different amounts of water and various temperatures (100−150 °C). Without the addition of water, the Th−H_2bdc−DMF system gives rise to the formation of two phases, $Th(bdc)_2(DMF)_2$ (**1**) and $Th_6O_4(OH)_4(H_2O)_6(bdc)_6{\cdot}6DMF{\cdot}12H_2O$ (**3**) (bdc = 1,4-benzenedicarboxylate or terephthalate). Their structures are built up of isolated thorium centers $ThO_8(DMF)_2$ for (**1**) and the hexanuclear core $Th_6O_4(OH)_4(H_2O)_6$ for (**3**). The latter adopts the UiO-66 metal−organic framework topology and exhibits a very high porosity for an actinides-based porous material (BET surface up to 730(6) $m^2{\cdot}g^{-1}$). The synthesis of (**3**) is also favored upon adding water. However, for pure aqueous solutions or for a very low amount of water, a third solid $Th(bdc)_2$ (**2**) crystallizes and contains thorium monomers ThO_8. The main similitude with the parent system dedicated to tetravalent uranium concerns the possibility to stabilize the $An_6O_8(H_2O)_6$ core by terephthalate linkers and to reproduce $An(bdc)_2(DMF)_2$ for both actinides U^{4+} and Th^{4+}. The thermal treatment of the latter shows a structural transition into the crystalline $Th(bdc)_2$ (**2**) solid.

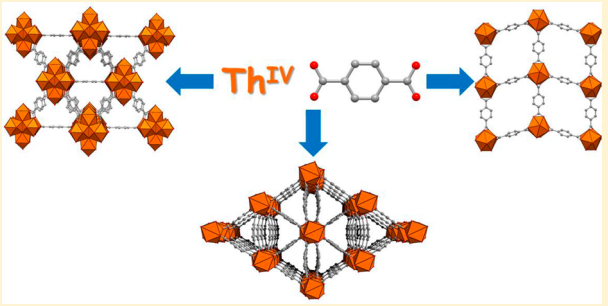

INTRODUCTION

The chemistry of coordination polymers represents a wide field for the elaboration of new hybrid organic−inorganic materials together with the opportunity to discover new structural topologies. For example, the crystalline structures of porous coordination polymers (also known as metal−organic framework) cover a large variety of metal−carboxylates clusters, from mononuclear subunits up to infinite chains or polyoxometallates blocks.[1−3]

The family of actinides also benefited from this enthusiasm for the discovery of new chemical architectures. The majority of these works was dedicated to the use of the dioxo uranyl cation, which combines a relatively moderate radiotoxicity (for the natural isotope ^{238}U) and a good stability under ambient conditions.[4,5] This approach led to the identification of a wide diversity of structures, where uranyl species are inserted in different inorganic motifs in association with polytopic carboxylate ligands.[6−8] In spite of a relative rich library of structures, the chemistry of hexavalent uranium is restricted to a planar configuration due to the chemical feature of the uranyl cation, showing the two relatively inert trans $[UO_2]^{2+}$ bondings. Whereas the use of tetravalent actinides is less explored for the formation of coordination polymers, their strong Lewis acidity facilitates the formation of several clusters through hydrolysis and condensation processes.[9−11]

We recently initiate the stabilization of tetravalent uranium-based poly-oxo clusters by carboxylate ligands within molecular or multidimensional organization. Our approach is based on using solvothermal synthesis in organic solvent (THF, DMF) at moderate temperature (<150 °C) and the influence of the addition of a controlled amount of water to regulate the hydrolysis mechanisms. This method of synthesis allowed us the isolation of different structural motifs,[12−15] including a large U_{38} poly-oxo cluster.[16]

The same strategy was extended to the use of tetravalent thorium. We analyzed the reactivity of thorium chloride or nitrate with benzoic acid in a mixture of THF/H_2O under solvothermal conditions. This work led to the isolation of two thorium benzoate polytypes, consisting of the similar assembly of infinite chains of square antiprismatic units ThO_8.[17] Other works previously reported the synthesis and structural features of thorium carboxylates involving diverse aromatic or aliphatic polytopic linkers,[18−25] some of them exhibiting open-framework structures.[26,27]

Here, we continue our investigations dedicated to thorium-based coordination polymers and analyzed the reactivity of terephthalic acid (H_2bdc) with this actinide, under solvothermal conditions in DMF, with a controlled addition of water. Three different phases were isolated, from the control of three synthesis parameters: temperature, Th/bdc molar ratio, and the concentration of water. They correspond to $Th(bdc)_2(DMF)_2$ (**1**), $Th(bdc)_2$ (**2**), and $Th_6O_4(OH)_4(H_2O)_6(bdc)_6{\cdot}6DMF{\cdot}12H_2O$ (**3**). Compounds **1** and **3** are similar to their tetravalent

Received: November 13, 2014
Published: February 10, 2015

DOI: 10.1021/ic502725y
Inorg. Chem. 2015, 54, 2235−2242

Table 1. Crystal Data and Structure Refinement for Thorium Terephthalates

	1	2	3
formula	$C_{22}H_{22}N_2O_{10}Th$	$C_{16}H_8O_8Th$	$C_{48}H_{24}O_{38}Th_6$
formula weight	706.46	560.26	2600.91
temperature/K	293	293	293
crystal color	colorless	colorless	yellowish
crystal size/mm	0.09 × 0.05 × 0.04	0.19 × 0.11 × 0.07	0.15 × 0.10 × 0.06
crystal system	monoclinic	monoclinic	cubic
space group	$C2/c$	$C2/c$	$Fm\bar{3}m$
a/Å	15.3843(2)	11.5931(2)	21.9606(13)
b/Å	11.5872(1)	18.0521(3)	21.9606(13)
c/Å	13.4949(2)	9.1948(2)	21.9606(13)
α/deg	90	90	90
β/deg	101.713(1)	114.457(1)	90
γ/deg	90	90	90
volume/Å^3	2355.52(5)	1751.62(6)	10590.9(11)
Z, $\rho_{calculated}$/g·cm^{-3}	4, 1.992	4, 2.125	4, 1.631
μ/mm^{-1}	6.390	8.552	8.45
Θ range/deg	2.22−30.51	2.24−28.32	1.61−30.44
limiting indices	$-21 \le h \le 21$	$-15 \le h \le 15$	$-26 \le h \le 23$
	$-16 \le k \le 16$	$-24 \le k \le 22$	$-17 \le k \le 31$
	$-19 \le l \le 19$	$-12 \le l \le 12$	$-31 \le l \le 28$
collected reflections	29 179	15 549	15 897
unique reflections	3598	2193	873
	[R(int) = 0.0530]	[R(int) = 0.0357]	[R(int) = 0.0335]
parameters	161	114	30
goodness-of-fit on F^2	1.069	1.303	1.320
final R indices [$I > 2\sigma(I)$]	R1 = 0.0242	R1 = 0.0141	R1 = 0.0293
	wR2 = 0.0531	wR2 = 0.0376	wR2 = 0.1154
R indices (all data)	R1 = 0.0318	R1 = 0.0173	R1 = 0.0330
	wR2 = 0.0557	wR2 = 0.0599	wR2 = 0.1183
largest diff. peak and hole/e·Å^{-3}	1.51 and −0.86	1.15 and −1.15	2.18 and −0.95

uranium analogues, $U(bdc)_2(DMF)_2$[12] and $U_6O_4(OH)_4(H_2O)_6(bdc)_6$·6DMF·12$H_2O$.[12,14] The structure of **3** is identical to the UiO-66 topology initially generated with zirconium.[28] This contribution deals with the synthesis and structural characterization (XRD, IR, TG, BET) of the compounds **1**−**3**. The thermal structural transformation of the phase $Th(bdc)_2(DMF)_2$ (**1**) into phase $Th(bdc)_2$ (**2**) is detailed. A discussion related to the composition diagram is also given for the chemical system Th−H_2bdc−DMF−H_2O.

EXPERIMENTAL SECTION

Synthesis. ***Caution!*** *Thorium nitrate ($Th(NO_3)_4$·5H_2O) is a radioactive and chemically toxic reactant, so precautions with suitable care and protection for handling such substances have been followed.*

The compounds have been solvothermally synthesized under autogenous pressure using 23 mL Teflon-lined Parr type autoclaves (type 4746) by using the following chemical reactants: thorium nitrate ($Th(NO_3)_4$·5H_2O, Fluka, 99%), terephthalic acid (1,4-benzenedicarboxylic acid or H_2bdc, Aldrich 99%), anhydrous *N*,*N*-dimethylformamide (noted DMF, Aldrich, 99.8%), and deionized water.

$Th(bdc)_2(DMF)_2$ (**1**): a mixture containing 200 mg (0.35 mmol) of $Th(NO_3)_4$·5H_2O, 150 mg (0.9 mmol) of terephthalic acid, and 5 mL (64 mmol) of *N*,*N*-dimethylformamide was placed in a Parr autoclave and then heated statically at 130 °C for 24 h. The resulting white product was then filtered off, washed with *N*,*N*-dimethylformamide, and dried at room temperature in an air atmosphere. It gives crystallites with a specific parallelepiped shape of 20−150 μm, as it can be observed by SEM (Figure S1a, Supporting Information).

$Th(bdc)_2$ (**2**): a mixture containing 200 mg (0.35 mmol) of $Th(NO_3)_4$·5H_2O, 150 mg (0.9 mmol) of terephthalic acid, and 5 mL (277 mmol) of H_2O was placed in a Parr autoclave and then heated statically at 150 °C for 36 h. The resulting white product was then filtered off, washed with *N*,*N*-dimethylformamide, and dried at room temperature in an air atmosphere. It gives crystallites (yield: 72%) with a specific parallelepiped shape of 20−150 μm, as it can be observed by SEM (Figure S1b, Supporting Information).

$Th_6O_4(OH)_4(H_2O)_6(bdc)_6$·6DMF·12$H_2O$ (**3**): a mixture containing 200 mg (0.35 mmol) of $Th(NO_3)_4$·5H_2O, 150 mg (0.9 mmol) of terephthalic acid, 4 mL (51 mmol) of *N*,*N*-dimethylformamide, and 1 mL (55 mmol) of H_2O was placed in a Parr autoclave and then heated statically at 130 °C for 36 h. The resulting white product was then filtered off, washed with *N*,*N*-dimethylformamide, and dried at room temperature in an air atmosphere (yield: 88%). With this synthetic procedure, it was not possible to get suitable single crystals for further X-ray diffraction analysis. In fact, we used another synthesis batch, for which the major phase was $Th(bdc)_2$ (**2**) and impurities of **3** appeared as relatively large crystals. The mixture of the starting reactants was 200 mg (0.35 mmol) of $Th(NO_3)_4$·5H_2O, 150 mg (0.9 mmol) of terephthalic acid, and 5 mL (277 mmol) of distilled water, which was placed in a Parr autoclave and then heated statically at 130 °C for 36 h. The resulting yellowish product was then filtered off, washed with DMF, and dried at room temperature. It gives crystallites with a specific octahedral shape of 20−150 μm, as it can be observed by SEM (Figure S1c, Supporting Information).

Single-Crystal X-ray Diffraction. Crystals of compounds **1**−**3** were selected under a polarizing optical microscope and glued on a glass fiber for a single-crystal X-ray diffraction experiment. X-ray intensity data were collected on a Bruker X8-APEX2 CCD area-detector diffractometer using Mo-K_α radiation (λ = 0.71073 Å) with an optical fiber as collimator. Several sets of narrow data frames (20 s per frame) were collected at different values of θ for 2 and 2 initial values of ϕ and ω, respectively, using 0.3° increments of ϕ or ω. Data reduction was accomplished using SAINT V7.53a.[29] The substantial

DOI: 10.1021/ic502725y
Inorg. Chem. 2015, 54, 2235−2242

redundancy in data allowed a semiempirical absorption correction (SADABS V2.10[30]) to be applied, on the basis of multiple measurements of equivalent reflections. The structure was solved by direct methods, developed by successive difference Fourier syntheses, and refined by full-matrix least-squares on all F^2 data using the SHELX suite program.[31] Hydrogen atoms of the benzene ring were included in calculated positions and allowed to ride on their parent atoms. The final refinements include anisotropic thermal parameters of all non-hydrogen atoms. The crystal data are given in Table 1. Supporting Information is available in CIF format.

X-ray Thermodiffraction. X-ray thermodiffractometry was performed for compounds **1**−**3** under 5 L·h^{-1} air flow in an Anton Paar HTK1200N of a D8 Advance Bruker diffractometer (θ−θ mode, Cu$K_{\alpha1/\alpha2}$ radiation) equipped with a Vantec1 linear position sensitive detector (PSD). Each powder pattern was recorded in the range of 6−60° (2θ) (at intervals of 20 °C between RT and 800 °C) with a 1 s/step scan, corresponding to an approximate duration of 27 min. The temperature ramps between two patterns were 5 °C·min^{-1}.

Infrared Spectroscopy. Infrared spectra of the powdered compounds **1**−**3** (see the Supporting Information) were measured on a PerkinElmer Spectrum Two spectrometer between 4000 and 400 cm^{-1}, equipped with a diamond attenuated total reflectance (ATR) accessory. Thermal behavior of compound **3** was characterized by in situ IR spectroscopy in air, with a heating rate of 10 °C·min^{-1} from RT up to 210 °C. During this period, 197 spectra were recorded in the range of 4000−400 cm^{-1}, with a resolution of 4 cm^{-1}, on a PerkinElmer Spectrum Two spectrometer equipped with a Pike Special-IR GladiATR accessory.

Thermogravimetric Analysis. The thermogravimetric experiments have been carried out for the phases **1**−**3**, on a thermoanalyzer TGA 92 SETARAM under air atmosphere with a heating rate of 10 °C·min^{-1} from room temperature up to 800 °C.

Surface Area Measurement. The porosity of compound **3** was estimated by gas sorption isotherm experiment in liquid nitrogen using the Micromeritics ASAP2020 apparatus. Before sorption measurements, the sample was outgassed under primary vacuum (5 Pa) at 200 °C for 15 h.

RESULTS

Structure Descriptions. The structure of Th(bdc)$_2$(DMF)$_2$ (**1**) is similar to that of the actinide terephthalate bearing tetravalent uranium.[12] It consists of one unique crystallographic metallic center, with a 10-fold coordination environment. The thorium atom is coordinated by eight carboxyl oxygen atoms from four distinct terephthalate linkers and two carbonyl oxygen atoms from two distinct *N*,*N*-dimethylformamide (DMF) molecules (Figure 1). The Th−O^c (^{c} = carboxyl) bond distances are in the range of 2.500(2)−2.563(2) Å and the Th−O^f (^{f} = carbonyl) bond distance is 2.406(2) Å. Such typical Th−O bond lengths have been previously reported in other thorium oxalates[32−35] containing a 10-fold coordinated metallic center. The two DMF species are located in a *trans* position within the coordination sphere of the thorium center. The therephthalate ligands adopt a chelating connection mode, with the positions of the carbon atoms of each carboxylate groups, situated in a perpendicular square plane. The orientation of three of the carboxylate arms is perpendicular to the previously defined square plane (from carbon nodes), whereas the orientation of the fourth carboxylate arm is parallel to this square plane. The ditopic character of terephthalate induces the generation of infinite layers of $ThO_8(DMF)_2$ units, connected to each other through the organic ligands. The resulting neutral sheets, [Th(bdc)$_2$(DMF)$_2$], are developed perpendicularly to the [101] direction (Figure 2) and are defined by a distorted square 4^4 net. The DMF molecules are pointed upward and downward the layer

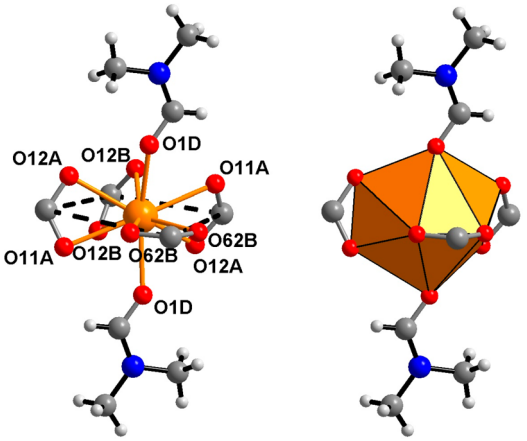

Figure 1. Coordination environments around the metallic center in Th(bdc)$_2$(DMF)$_2$ (**1**). The square plane is defined by the four carbon centers of the each carboxylate arm of the terephthalate, and indicated by the dotted line. Aromatic rings are omitted for clarity. The *N*,*N*-dimethylformamide is located at the apical position of the ThO_8-(DMF)$_2$ polyhedron.

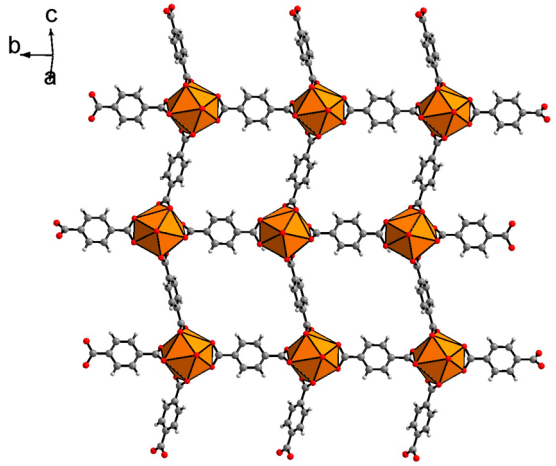

Figure 2. View of the neutral layer in Th(bdc)$_2$(DMF)$_2$ (**1**) along the [101] direction. *N*,*N*-Dimethylformamide molecules are pointing upward and downward the plane of the layers along [101]. Orange polyhedra correspond to one given organic−inorganic sheet.

and prevent any connection between the thorium centers for the formation of a three-dimensional framework. The cohesion of the structure is ensured through van der Waals interactions, by the stacking of the layers along the [101] direction, with a shift of (a + b)/2 from one to the adjacent others. As mentioned for the parent compound with tetravalent uranium,[12] the arrangement is closely related to that of a sodium-lanthanum terephthalate, Na[La(bdc)$_2$(DMF)$_2$],[36] incorporating *N*,*N*-dimethylformamide species, within the 10-fold coordinated La centers. In the latter compound, the structure is three-dimensional, due to the presence of sodium cations, which ensures the connection of the anionic layers [La(bdc)$_2$-(DMF)$_2$]$^-$ to each others.

The presence of connected DMF molecules is also established by infrared spectroscopy (Figure S5a, Supporting Information), thanks to the peak centered at 1642 cm^{-1}, corresponding to the amide function ν(C═O) of this solvent. In the range of 1600−1300 cm^{-1}, other bands can be assigned to carboxylate functions (ν_{asym}(COO) = 1553 cm^{-1},

DOI: 10.1021/ic502725y
Inorg. Chem. 2015, 54, 2235−2242

ν_{sym}(COO) = 1411 and 1368 cm^{-1}) or aromatic C═C bonds from the ligand (ν(C═C) = 1508 cm^{-1}).

The structure of compound **2** (Th(bdc)$_2$) contains the same Th/bdc molar ratio compared to **1**, but no DMF species is present. The thorium coordination is thus reduced to eight oxygen atoms coming from the carboxylate function of the terephthalate ligand. The Th−O^c bond distances are ranging from 2.358(3) to 2.439(3) Å, defined by a distorted Archimedean square antiprismatic polyhedron, ThO$_8$ (Figure 3). The thorium atoms are linked to other through the

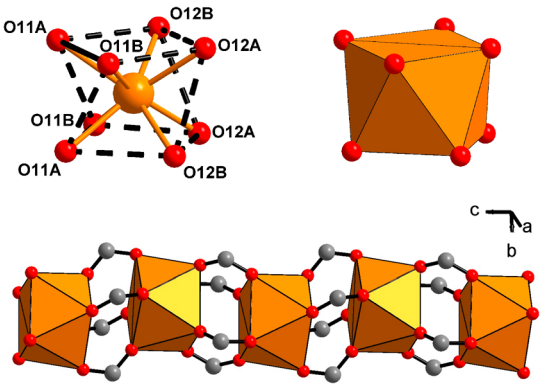

Figure 3. (top) Representation of the 8-fold coordinated thorium with a antiprismatic geometry (ThO$_8$) in Th(bdc)$_2$ (**2**). (bottom) View of the connection mode of the ThO$_8$ polyedral units through the carboxylate arm of the terephthalate ligands, generating an infinite chain running along the *c* axis.

carboxylate arms acting as *syn*−*syn* bidentate bridges. In this connection mode, two adjacent thorium centers are linked via carboxylate groups from four distinct terephthalate ligands. The bidentate connection is ensured by four oxygen atoms belonging to the two adjacent square faces of two neighboring square antiprismatic polyhedra. It results in the formation of infinite chains of ThO$_8$ polyhedra, developed along the *c* axis. A similar subunit has been previously described in 1D coordination polymers obtained with benzoic acid in Th(benzoate)$_4$.[17] This particular 8-fold environment for thorium has been also reported in different inorganic phases[37−40] or organic−inorganic complexes.[41] The connection of the ThO$_8$ polyhedra with the terephthalate linker generates a 3D framework (Figure 4) delimiting a triangular net in the (*a*,*b*) plane, with narrow tunnels running along the axis of the chains

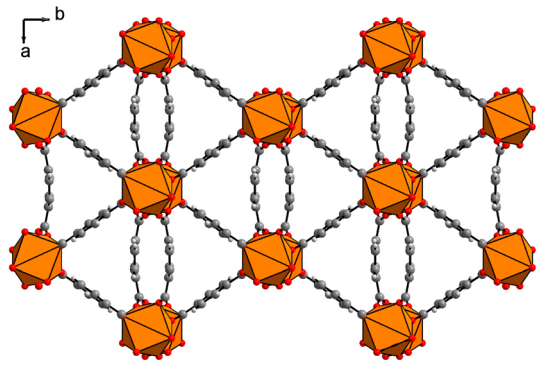

Figure 4. View of the structure of Th(bdc)$_2$ (**2**) along the *c* axis, showing the connection mode of the chain of ThO$_8$ polyhedral units through the terephthalate ligand, resulting in a 3D network.

(*c*). Due to the steric hindrance of oxygen and carbon atoms defining channels, the calculated remaining free pore diameter is around 2 Å.

The infrared spectrum of **2** (Figure S5b, Supporting Information) confirms the absence of a water molecule within the structure, since no absorption band is observable in the 3600−2500 cm^{-1} range. The asymmetric ν_{asym}(COO) and the symmetric vibrations ν_{sym}(COO) associated with the carboxylate function are localized at 1551 and 1392 cm^{-1}, respectively. The peak centered at 1500 cm^{-1} corresponds to the C−C vibrations related to the benzene ring. A very low vibration at 1661 cm^{-1} could indicate the adsorption of traces of DMF ν(C═O) at the solid surface, during the filtration process.

The third phase ($Th_6O_4(OH)_4(H_2O)_6(bdc)_6$·6DMF·12$H_2O$, **3**) observed in the Th−bdc−DMF system is related to the well-known series with the UiO-66 topology reported with tetravalent transition metals such as zirconium[28] or hafnium.[42] Its crystal structure is composed of hexanuclear inorganic subunits, containing 9-fold coordinated thorium centers with a monocapped square antiprismatic geometry (Figure 5). There

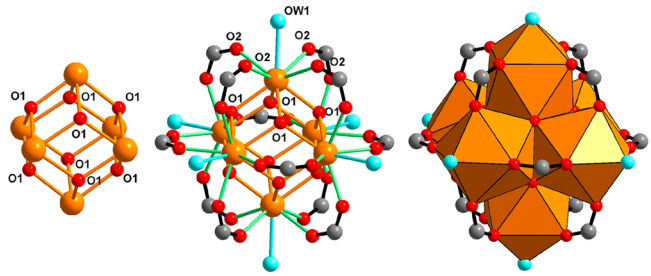

Figure 5. Views of the hexanuclear core in $Th_6O_4(OH)_4(H_2O)_6(bdc)_6$·6DMF·12$H_2O$ (**3**). (left) "$Th_6O_4(OH)_4$" subunit; the oxo/hydroxo groups are disordered on the O1 positions. (middle) Ball-and-stick representation of the poly-oxo cluster [$Th_6O_4(OH)_4(H_2O)_6(O_2C-)_{12}$]. (right) Polyhedral representation of the poly-oxo cluster [$Th_6O_4(OH)_4(H_2O)_6(O_2C-)_{12}$]. Orange circles: thorium; red circles: oxygen; cyan circles: water.

are three types of oxygen atoms bound to thorium, within the hexameric cluster. Four of them correspond to carboxyl oxygen atoms with a Th−O2 bond distance of 2.454(5) Å and define one of the two square faces of the antiprismatic polyhedron. Four other oxygen atoms adopt a bridging mode between three thorium centers with a μ_3 configuration and are situated at each corner of the second square face of the antiprismatic polyhedron. The corresponding Th−O1 bond distance is 2.415(6) Å. The ninth oxygen atom (Ow) is assigned to a terminal water molecule with a slightly longer bond distance of 2.650(15) Å. It results in the formation of a hexanuclear core "$Th_6O_8(H_2O)_6$", for which the positions of the thorium cations are located at the corner of an octahedron. Such a poly-oxo cluster is quite common for the crystal chemistry of thorium, or more generally for tetravalent actinides. It has been reported in other carboxylates such as formate,[18,20] acetate,[20] or glycine[19,43] complexes bearing thorium. Other occurrences of this specific hexameric unit have been encountered with uranium,[10,13,14,18,44] neptunium,[45] or plutonium,[46] under their tetravalent oxidation state. In compound **3**, the inorganic cores are linked to other through the ditopic ligands, via the carboxylate groups, which bridge two thorium centers in a *syn*−*syn* bidentate mode. The resulting structure is built up from the three-dimensional connection of such hexamers and tereph-

DOI: 10.1021/ic502725y
Inorg. Chem. 2015, 54, 2235−2242

thalate linkers, giving rise to the generation of a cubic topology with the fcc packing (Figure 6). In such an arrangement, the

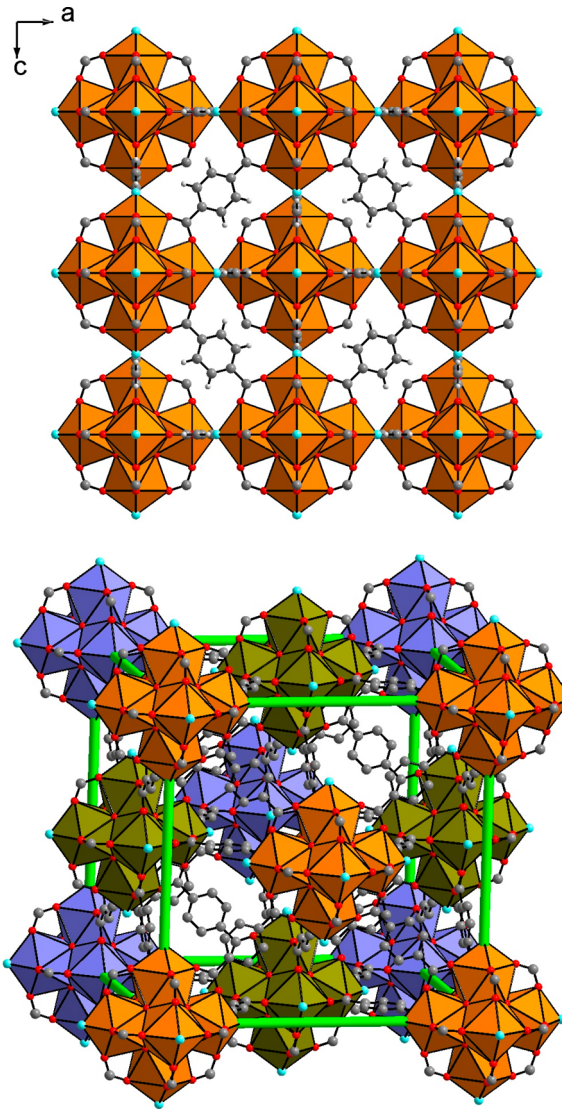

Figure 6. (top) View of the structure of $Th_6O_4(OH)_4(H_2O)_6(bdc)_6 \cdot 6DMF \cdot 12H_2O$ (**3**) in the (*a*,*c*) plane. (bottom) Perspective view of the cubic cell of **3**. Different colors of the hexanuclear poly-oxo cluster are indicated for clarity.

hexameric units play the role of nodes delimiting tetrahedral or octahedral cavities (Figure 7). A similar structure has been obtained recently with tetravalent uranium with different ditopic ligands (fumarate, 2,6-napthalenedicarboxylate, 4,4′-biphenyldicarboxylate).[13,14] From the X-ray diffraction study, the deduced chemical formula of the organic–inorganic 3D framework is "$[Th_6O_8(H_2O)_6(bdc)_6]$", and four of the μ_3-oxygen atoms must correspond to hydroxo groups in order to the balance the electroneutrality of the crystal structure. In fact, the presence of μ_3-O or μ_3-OH species should be observed by X-ray diffraction analysis, with contrasted Th–O distances. For instance, in the Th–glycine complex,[43] the Th–μ_3O bond value is 2.291(10) Å, whereas the Th–μ_3OH bond value is 2.502(8) Å. In our case, only an average Th–μ_3(O,OH) bond distance of 2.415(6) Å is observed, due to the high symmetry of the cubic crystal ($Fm\bar{3}m$). The assignment of oxo/hydroxo to the μ_3-oxygen bridging positions is a recurrent issue in this type

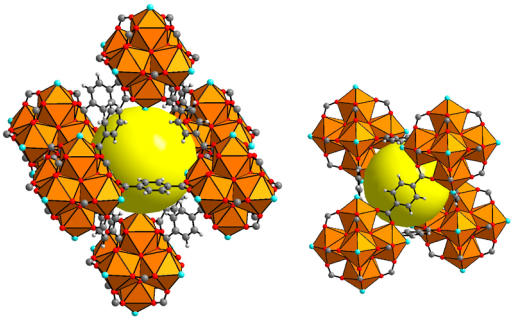

Figure 7. Views of the octahedral (left) and tetrahedral (right) cavities in $Th_6O_4(OH)_4(H_2O)_6(bdc)_6 \cdot 6DMF \cdot 12H_2O$ (**3**).

of complexes, described in high symmetric crystal systems, and O/OH disordering has been previously reported for the μ_3-bridging species in other compounds.[18,20]

The sizes of the octahedral and tetrahedral cavities are 10.0 and 3.0 Å, respectively (Figure 7). The examination of the difference Fourier map did not reveal any clear positions of the encapsulated species within the different cages, but elemental analysis was in good agreement with the presence of free DMF and water molecules within the pores. In fact, about 6 DMF and 12 water molecules per "Th_6" subunit have been found (C: obs.: 24.24%, calc.: 24.22%; H: obs.: 2.67%; calc.: 3.24%; N: obs.: 1.92%, calc.: 2.56%).

The pore loading by DMF is also observable by infrared spectroscopy (Figure S5c, Supporting Information) through a peak at 1660 cm^{-1} (ν(C═O)) and a doublet localized at 2928 cm^{-1} (ν(C-H)). The absence of a peak around 1700 cm^{-1} indicates that free terephthalic acid is not contained within the pores. The infrared signature of the coordinated ligand is revealed by three specific peaks at 1586, 1398, and 1503 cm^{-1}, corresponding to the vibration of the carboxylate functions (ν_{asym}(COO) and ν_{sym}(COO)) and the benzene ring (ν (C═C)), respectively. The broad band centered at 3350 cm^{-1} covers the vibrations of O–H bonds coming from water and terminal hydroxyl groups connected to the uranium cluster. In the temperature range of RT–210 °C, the thermal in situ infrared analysis of **3** (Figure S7, Supporting Information) indicates that the departure of water makes visible a relative broad peak centered at 3600 cm^{-1}, which is assigned to the terminal hydroxyl functions.

The porosity properties have been estimated from the adsorption of nitrogen at 77 K. The sorption experiment (Figure S6, Supporting Information) on the activated phase **3** revealed a type I isotherm with a plateau at 200 $cm^3 \cdot g^{-1}$, which is characteristic of a microporous solid. The activation process consists of heating the as-synthesized product at 200 °C overnight. The measured Brunauer–Emmett–Teller (BET) surface area was estimated to be 730(6) $m^2 \cdot g^{-1}$ (within the range $0.017 < p/p_0 < 0.15$) with a micropore volume of 0.27 $cm^3 \cdot g^{-1}$, and assuming a monolayer coverage by nitrogen, the Langmuir surface area is 868(3) $m^2 \cdot g^{-1}$. For comparison, no BET/Langmuir surface was measured for the uranium-based analogous compound, due to the poor stability of the framework.[14] The zirconium-based phase (UiO-66) showed a Langmuir surface of 1187 $m^2 \cdot g^{-1}$.[28]

DISCUSSION

The analysis of the chemical system involving thorium, terephthalic acid, and a controlled amount of water in *N*,*N*-

DOI: 10.1021/ic502725y
Inorg. Chem. 2015, 54, 2235–2242

dimethylformamide revealed the occurrence of three distinct phases in the temperature range of 120−150 °C and different bdc/Th or H_2O/Th molar ratios (Figure 8). In the absence of water addition, the major phase is $Th(bdc)_2(DMF)_2$ (**1**), which exhibits thorium with a 10-fold coordination composed of eight carboxyl oxygen atoms (from terephthalate ligand) and two carbonyl oxygen atoms (from DMF molecules). This compound crystallized for a molar ratio of bdc/Th ranging from 1 up to 4, and for a temperature from 120 up to 150 °C. However, the system is not totally anhydrous since the thorium source was used under its hydrated form ($Th(NO_3)_4{\cdot}5H_2O$). The presence of the water has a direct influence on the formation of the UiO-66 analogous phase ($Th_6O_4(OH)_4(H_2O)_6(bdc)_6{\cdot}6DMF{\cdot}12H_2O$, **3**), since it consists of hexanuclear clusters as secondary building units, with the occurrence of μ_3-O and μ_3-OH bridges between thorium centers. The latter reflect that olation/oxolation hydrolysis reactions took place during the solvothermal treatment, in order to form Th−O−Th and Th−OH−Th bondings, for the generation of polynuclear motifs. The phase **3** is present at relatively low temperature (120 °C) or in a mixture with **1** when increasing the temperature, for a bdc/Th molar ratio of 1/1. If the bdc/Th molar ratio is higher than 1, the phase **3** disappeared and the crystallization of anhydrous phase **1** is favored. In the same temperature range, the addition of water to the reactants mixture gave rise to the formation of the phase **3**, which is still present in a purely water system (H_2O/Th = 795, DMF is not present). However, a third phase ($Th(bdc)_2$, **2**) is observed in the hydrothermal conditions, when the temperature is increased. It is only built from discrete mononuclear 8-fold coordinated thorium cations.

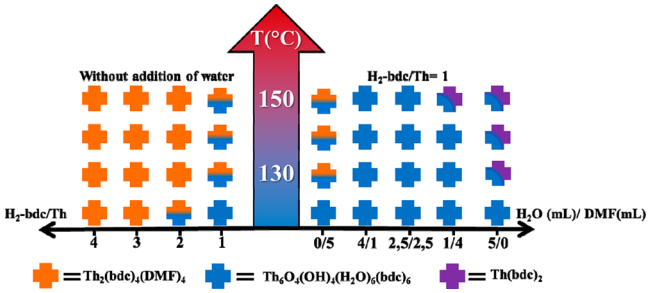

Figure 8. Composition diagram of the chemical system Th−bdc−DMF−H_2O, showing the domains of occurrence of the three phases: $Th(bdc)_2(DMF)_2$ (**1**), $Th(bdc)_2$ (**2**), and $Th_6O_4(OH)_4(H_2O)_6(bdc)_6{\cdot}6DMF{\cdot}12H_2O$ (**3**).

At first sight, it seems surprising that this last phase does not exhibit oxo or hydroxo groups in a thorium coordination sphere, instead of a high concentration of water and relative high temperature. The organization observed in **2** could suggest the influence of DMF for the cation hydrolysis process. Indeed, the decomposition of DMF and the possible production of dimethylamonium cation[47−50] could produce relative basic conditions favorable to formation of hydrolyzed thorium. This would be related to the wide domain of occurrence of the phase **3**, exhibiting a hexanuclear motif with O/OH bridging groups between the thorium centers. In the absence of DMF, only a coordination polymer with isolated thorium centers is observed (phase **2**).

Similar investigations have been studied with tetravalent uranium and the same additional components (terephthalic acid, *N*,*N*-dimethylformamide, and water).[12] The analogous phases **1** and **3** have been isolated in similar conditions (anhydrous/hydrous, respectively), but one of the main differences is the chemical behavior against hydrolysis, related to the amount of water. With thorium, only the compound $Th_6O_4(OH)_4(H_2O)_6(bdc)_6{\cdot}6DMF{\cdot}12H_2O$ (**3**) is present in a wide domain of H_2O/Th molar ratios (5−795), and also in a purely water system. With uranium, the existence domain of such a phase was much more limited since it crystallized for H_2O/U molar ratios between 2 and 15. Above the value of H_2O/U = 15, only the formation of urania UO_2 was observed, whereas the equivalent phase thoria, ThO_2, was not visible at all. This other point is the formation at higher temperature, of another compound, $U_2O_2(bdc)_2(DMF)$, characterized by chains of uranium centers with μ_3-oxo bridges, in the presence of water (H_2O/U = 2−10). This phase showed a higher order of condensation with the generation of infinite ···U−O−U·· bondings. With thorium, the increase of temperature led to the crystallization in water, of another phase $Th(bdc)_2$ (**2**), which did not exhibit any oxo brigding ligands since only isolated ThO_8 polyhedral units are observed in the crystal structure. The last distinct point is the formation of the two polytypes $U_2Cl_2(bdc)_3(DMF)_4$, for a low bdc/U molar ratio. The latter were not observed in the case of thorium.

The analysis of the two composition diagrams with Th^{4+} or U^{4+} showed distinct chemical behaviors, which may reflect the subtle difference of the Lewis acidity for these two actinides.[9] Thorium is known to be less acidic (Lewis) compared to uranium, and olation condensation reaction is favored against oxolation reactions. For uranium, which is slightly more acidic, condensation reaction would preferentially occur through oxolation, with the formation of U−O−U bonding. This fact

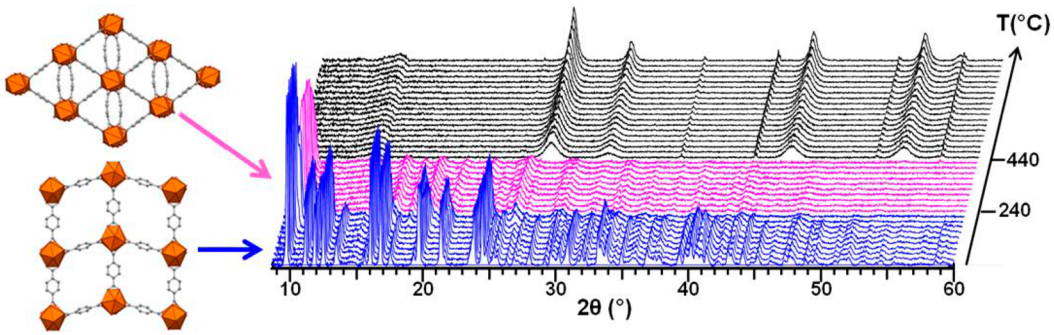

Figure 9. Powder X-ray diffraction patterns as a function of temperature (2θ; copper radiation) showing the structural transformation of $Th(bdc)_2(DMF)_2$ (**1**) into $Th(bdc)_2$ (**2**) from 240 °C.

DOI: 10.1021/ic502725y
Inorg. Chem. 2015, 54, 2235−2242

is observed with the formation of a $U_2O_2(bdc)_2(DMF)$ compound (infinite chains) or the favored formation of uranium UO_2, for a relatively low H_2O/U molar ratio, whereas the phase ThO_2 is not observed in our conditions. Moreover, a chain-like is obtained for higher temperature with thorium ($Th(bdc)_2$), but without any Th−O−Th bonding.

Thermal Behavior. The three phases have been characterized by thermogravimetric analyses. For compound **1**, the TG curve (Figure S4a, Supporting Information) shows a weight loss with two steps. The first event (obs.: 20.5%) occurs between 200 and 270 °C and is assigned to the departure of two DMF molecules (calc.: 20.7%). Then, a continuous weight loss is observed together with the decomposition of the organic linker between 430 and 470 °C. From 470 °C, the remaining weight is 38.8% from 470 °C (calc.: 37.4%) and the basis of ThO_2, as the final residue. For compound **2** (Figure S4b, Supporting Information), one observed only one single step for the weight loss process, which occurred from 500 °C. The remaining weight is 47.9% (calc.: 47.2%) on the basis of ThO_2.

The thermal decomposition of **3** (Figure S4c, Supporting Information) reveals a first weight loss between 20 and 80 °C, related to the departure of water molecules (obs.: 11.1%, calc.: 9.9%). In the range of 130−400 °C, a second transformation occurs and corresponds to the elimination of DMF from the pores (obs.: 12.2%, calc.: 13.4%). At 480 °C, we observe the collapse of the structure, and the final plateau is assigned to thorium oxide, ThO_2 (obs.: 47.8%, calc.: 48.4%).

The products have been analyzed by X-ray diffraction as a function of temperature up to 800 °C under an air atmosphere. The thermodiffractogram (Figure 9) of compound **1** indicated that the Bragg peaks persisted up to 240 °C. Then, a new powder XRD pattern appeared, assigned to a crystalline phase, which corresponds to the phase **2**, following the reaction:

$Th(bdc)_2(DMF)_2$ (**1**) → $Th(bdc)_2$ (**2**) + 2DMF from 240 °C. The latter is still visible up to 440 °C. It is interesting to notice the structural transformation of phase **1** into phase **2**, with the departure of the monondentate DMF ligand, together with the crystallization process. Here, the coordination state of thorium was 10-fold in phase **1** and 8-fold in phase **2**, due to the removal of DMF species. However, no direct relationship exists between the two phases since **1** possesses a bidimensional network and **2** has a tridimensional framework. This induces the Th−O−C bonds breaking and recombination in order to construct the structure of **2**, from that of **1**. The phase **2** is stable up to 440 °C, and then the Bragg peaks of the ThO_2 phase appeared from that temperature.

The diffractogram (Figure S3b, Supporting Information) of the as-synthesized compound **2** is closely related to the observation from TG analyses, with the Bragg peaks still visible up to 480 °C. Then, the crystallization of ThO_2 is observed.

For compound **3**, the thermal behavior was examined by in situ infrared between RT and 210 °C, in order to follow the departure of solvent molecules (Figure S7). At 60 °C, we identify the quick departure of water (broad band centered at 3600 cm^{-1}) and the appearance of a band at 3604 cm^{-1} corresponding to terminal hydroxyl groups. From 140 °C, the diminution of the peak at 1660 cm^{-1} highlights the departure of DMF. Between 140 and 210 °C, we observe new peaks at around 600 cm^{-1}, which could characterize the asymmetric stretching of the carboxylate function.[51]

CONCLUSION

In our systematic study dedicated to tetravalent-actinides based coordination polymers, this work showed the ability of thorium to react with terephthalic acid. The system mixing thorium nitrate hydrate, terephthalic acid, DMF, and water gave rise to the production and identification of three new crystalline phases. The investigations for their syntheses were conducted in the temperature range of 120−150 °C and different amounts of reactants with the molar ratios $5 < H_2O/Th < 800$ and $1 < H_2bdc/Th < 4$.

Without addition of water (excepted that from the hydrated thorium source), the system generates two phases, $Th_2(bdc)_4(DMF)_4$ and $[Th_6O_4(OH)_4(H_2O)_6(bdc)_6]$, which are both analogous to those previously obtained with tetravalent uranium.[12] It is interesting to note that the formation of the porous compound $[Th_6O_4(OH)_4(H_2O)_6(bdc)_6]$, derived from the UiO-66[28] type, needs a relative low amount of water, coming exclusively from the hydrated thorium nitrate salt. However, the increase in concentration of terephthalate ligand in the media generated the formation of $Th_2(bdc)_4(DMF)_4$.

The addition of water for a constant molar ratio of H_2bdc/Th equal to 1 confirms that this strategy favors an olation/oxolation condensation process and the stabilization of the hexameric cluster, exhibiting both oxo and hydroxo bridging groups.

Surprisingly, a very low amount or the absence of DMF favored the generation of the phase $Th(bdc)_2$. This structure was not previously observed with a uranium structure and does not demand an oxolation process. This last observation could indicate the importance of DMF in order to attain suitable conditions for cations hydrolysis. These conditions may be reached thanks to the decomposition of DMF in water and the apparition of a base (dimethylamine) in the medium.

The comparison with the parent system involving tetravalent uranium terephthalates[12]indicates the impossibility to reproduce the phase $U_2O_2(bdc)_2(DMF)$ with thorium. This last structure was constructed from infinite chains, in which metal centers are connected to each other via oxo groups. The fact that this structure was not accessible with thorium confirms the low affinity of this actinide for an infinite condensation process. Indeed, the occurrence of thoria, ThO_2, was not observed in our system, whereas the UO_2 phase is obtained when using tetravalent uranium.

In summary, this study is a rare example of the construction of thorium-based coordination polymers. As already observed with other actinides, the hydrolysis rate of thorium appears as a critical point for the control of cation condensation and the isolation of new architectures. Furthermore, the good stability and the potential porosity of the thorium-based structures (BET surface up to 730(6) $m^2 \cdot g^{-1}$) could be an opportunity to explore several properties like gas sorption or catalysis.

ASSOCIATED CONTENT

Supporting Information

SEM photographs, X-ray powder patterns, in situ X-ray diffractograms, thermogravimetric curves, IR spectra, nitrogen gas sorption isotherms, and CIF files. This material is available free of charge via the Internet at http://pubs.acs.org.

DOI: 10.1021/ic502725y
Inorg. Chem. 2015, 54, 2235−2242

AUTHOR INFORMATION

Corresponding Author

*E-mail: christophe.volkringer@ensc-lille.fr. Phone: (33) 3 20 434 973. Fax: (33) 3 20 43 48 95 (C.V.).

Notes

The authors declare no competing financial interest.

ACKNOWLEDGMENTS

The authors would like to thank Mrs. Nora Djelal, Laurence Burylo, Mr. Philippe Devaux for their assistance with the SEM images, XRD powder patterns, and TG measurements (UCCS). The "Fonds Européen de Développement Régional (FEDER)", "CNRS", "Région Nord Pas-de-Calais", and "Ministère de l'Education Nationale de l'Enseignement Supérieur et de la Recherche" are acknowledged for funding of X-ray diffractometers. C.F. acknowledges Université Lille 1 and "Région Nord Pas-de-Calais" for their Ph.D. grant support.

REFERENCES

(1) Tranchemontagne, D. J.; Mendoza-Cortes, J. L.; O'Keeffe, M.; Yaghi, O. M. *Chem. Soc. Rev.* **2009**, *38*, 1257.
(2) Ferey, G. *Chem. Soc. Rev.* **2008**, *37*, 191.
(3) Furukawa, S.; Reboul, J.; Diring, S.; Sumida, K.; Kitagawa, S. *Chem. Soc. Rev.* **2014**, *43*, 5700.
(4) Qiu, J.; Burns, P. C. *Chem. Rev.* **2013**, *113*, 1097.
(5) Burns, P. C. *Can. Mineral.* **2005**, *43*, 1839.
(6) Loiseau, T.; Mihalcea, I.; Henry, N.; Volkringer, C. *Coord. Chem. Rev.* **2013**, *266*−*267*, 69.
(7) Andrews, M. B.; Cahill, C. L. *Chem. Rev.* **2013**, *113*, 1121.
(8) Wang, K.-X.; Chen, J.-S. *Acc. Chem. Res.* **2011**, *44*, 531.
(9) Knope, K. E.; Soderholm, L. *Chem. Rev.* **2013**, *113*, 944.
(10) Nocton, G.; Burdet, F.; Pécaut, J.; Mazzanti, M. *Angew. Chem., Int. Ed.* **2007**, *46*, 7574.
(11) Biswas, B.; Mougel, V.; Pécaut, J.; Mazzanti, M. *Angew. Chem., Int. Ed.* **2011**, *50*, 5745.
(12) Falaise, C.; Assen, A.; Mihalcea, I.; Volkringer, C.; Mesbah, A.; Dacheux, N.; Loiseau, T. *Dalton Trans.* **2015**, *44*, 2639.
(13) Falaise, C.; Volkringer, C.; Loiseau, T. *Cryst. Growth Des.* **2013**, *13*, 3225.
(14) Falaise, C.; Volkringer, C.; Vigier, J.-F.; Henry, N.; Beaurain, A.; Loiseau, T. *Chem.—Eur. J.* **2013**, *19*, 5324.
(15) Volkringer, C.; Mihalcea, I.; Vigier, J.-F.; Beaurain, A.; Visseaux, M.; Loiseau, T. *Inorg. Chem.* **2011**, *50*, 11865.
(16) Falaise, C.; Volkringer, C.; Vigier, J.-F.; Beaurain, A.; Roussel, P.; Rabu, P.; Loiseau, T. *J. Am. Chem. Soc.* **2013**, *135*, 15678.
(17) Falaise, C.; Volkringer, C.; Loiseau, T. *Inorg. Chem. Commun.* **2014**, *39*, 26.
(18) Takao, S.; Takao, K.; Kraus, W.; Emmerling, F.; Scheinost, A. C.; Bernhard, G.; Hennig, C. *Eur. J. Inorg. Chem.* **2009**, 4771.
(19) Hennig, C.; Takao, S.; Takao, K.; Weiss, S.; Kraus, W.; Emmerling, F.; Scheinost, A. C. *Dalton Trans.* **2012**, *41*, 12818.
(20) Knope, K. E.; Wilson, R. E.; Vasiliu, M.; Dixon, D. A.; Soderholm, L. *Inorg. Chem.* **2011**, *50*, 9696.
(21) Ziegelruber, K. L.; Knope, K. E.; Frisch, M.; Cahill, C. L. *J. Solid State Chem.* **2008**, *181*, 373.
(22) Frisch, M.; Cahill, C. L. *Cryst. Growth Des.* **2008**, *8*, 2921.
(23) Ok, K. M.; O'Hare, D. *Dalton Trans.* **2008**, 5560.
(24) Thuéry, P. *Inorg. Chem.* **2011**, *50*, 1898.
(25) Ramaswamy, P.; Prabhu, R.; Natarajan, S. *Inorg. Chem.* **2010**, *49*, 7927.
(26) Ok, K. M.; Sung, J.; Hu, G.; Jacobs, R. M. J.; O'Hare, D. *J. Am. Chem. Soc.* **2008**, *130*, 3762.
(27) Kim, J. Y.; Norquist, A. J.; O'Hare, D. *J. Am. Chem. Soc.* **2003**, *125*, 12688.
(28) Hafizovic Cavka, J.; Jakobsen, S.; Olsbye, U.; Guilou, N.; Lamberti, C.; Bordiga, S.; Lillerud, K. P. *J. Am. Chem. Soc.* **2008**, *130*, 13850.
(29) *SAINT Plus*, Version 7.53a; Bruker Analytical X-ray Systems: Madison, WI, 2008.
(30) Sheldrick, G. M. *SADABS: Bruker-Siemens Area Detector Absorption and Other Correction*, Version 2008/1; University of Göttingen: Göttingen, Germany, 2008.
(31) Sheldrick, G. M. *Acta Crystallogr., Sect. A* **2008**, *64*, 112.
(32) Akhtar, M. N.; Smith, A. J. *Acta Crystallogr., Sect. B* **1975**, *31*, 1361.
(33) Clavier, N.; Hingant, N.; Rivenet, M.; Obbade, S.; Dacheux, N.; Barré, N.; Abraham, F. *Inorg. Chem.* **2010**, *49*, 1921.
(34) Andreev, G.; Budantseva, N.; Fedoseev, A.; Moisy, P. *Inorg. Chem.* **2011**, *50*, 11481.
(35) Zhang, Y.; Bhadbhade, M.; Karatchevtseva, I.; Gao, J.; Price, J. R.; Lumpkin, G. R. *Eur. J. Inorg. Chem.* **2013**, 6170.
(36) Long, L.-S.; Hu, J.-Y.; Ren, Y.-P.; Sun, Z.-G.; Huang, R.-B.; Zheng, L.-S. *Main Group Met. Chem.* **2002**, *25*, 749.
(37) Wallez, G.; Bregiroux, D.; Popa, K.; Raison, P.; Apostolidis, C.; Lindqvist-Reis, P.; Konings, J. M.; Popa, A. F. *Eur. J. Inorg. Chem.* **2011**, 110.
(38) Xiao, B.; Gesing, T. M.; Kegler, P.; Modolo, G.; Bosbach, D.; Schlenz, H.; Suleimanov, E. V.; Alekseev, E. V. *Inorg. Chem.* **2014**, *53*, 3088.
(39) Knope, K. E.; Wilson, R. E.; Skanthakumar, S.; Soderholm, L. *Inorg. Chem.* **2011**, *50*, 8621.
(40) Xiao, B.; Dellen, J.; Schlenz, H.; Bosbach, D.; Suleimanov, E. V.; Alekseev, E. V. *Cryst. Growth Des.* **2014**, *14*, 2677.
(41) Diwu, J.; Good, J. J.; DiStefano, V. H.; Albrecht-Schmitt, T. E. *Eur. J. Inorg. Chem.* **2011**, 1374.
(42) Jakobsen, S.; Gianolio, D.; Wragg, D. S.; Hellner Nilsen, M.; Emerich, H.; Bordiga, S.; Lamberti, C.; Olsbye, U.; Tilset, M.; Lillerud, K. P. *Phys. Rev. B* **2012**, *86*, 125429.
(43) Hu, Y.-J.; Knope, K. E.; Skanthakumar, S.; Soderholm, L. *Eur. J. Inorg. Chem.* **2013**, 4159.
(44) Mougel, V.; Biswas, B.; Pécaut, J.; Mazzanti, M. *Chem. Commun.* **2010**, *46*, 8648.
(45) Takao, K.; Takao, S.; Scheinost, A. C.; Bernhard, G.; Hennig, C. *Inorg. Chem.* **2012**, *51*, 1336.
(46) Knope, K. E.; Soderholm, L. *Inorg. Chem.* **2013**, *52*, 6770.
(47) Thuery, P.; Harrowfield, J. *Cryst. Growth Des.* **2014**, *14*, 1314.
(48) Thuery, P. *Cryst. Growth Des.* **2012**, *12*, 499.
(49) Thuery, P. *Cryst. Growth Des.* **2011**, *11*, 2606.
(50) Mihalcea, I.; Henry, N.; Loiseau, T. *Eur. J. Inorg. Chem.* **2014**, 1322.
(51) Valenzano, L.; Civalleri, B.; Chavan, S.; Bordiga, S.; Nilsen, M. H.; Jakobsen, S.; Lillerud, K. P.; Lamberti, C. *Chem. Mater.* **2011**, *23*, 1700.

DOI: 10.1021/ic502725y
Inorg. Chem. 2015, 54, 2235−2242